

Improved nonsinglet QCD analysis of the fixed-target DIS data

A.V. Kotikov, V.G. Krivokhizhin, B.G. Shaikhatdenov
 Joint Institute for Nuclear Research, Russia

October 18, 2018

Abstract

Deep inelastic scattering data on F_2 structure function obtained by BCDMS, SLAC and NMC collaborations in fixed-target experiments are analyzed in the non-singlet approximation with next-to-next-to-leading-order accuracy. The strong coupling constant is found to be $\alpha_s(M_Z^2) = 0.1157 \pm 0.0022$ (total exp.error) + $\begin{cases} +0.0028 \\ -0.0016 \end{cases}$ (theor), which is seen to be well compatible with the average world value. The results, obtained in the present paper by carrying out fits similar to what were performed in [1], with the exception for systematic errors in BCDMS data taken into account in a different way, confirm our previous ones derived in [1]. This study is also meant to at least partially explain differences in the latest predictions for LHC observables, caused by usage of different sets of parton distribution functions obtained by different groups.

PACS : 12.38 Aw, Bx, Qk

Keywords: Deep inelastic scattering; Nucleon structure functions; QCD coupling constant; NNLO level; $1/Q^2$ power corrections.

1 Introduction

The cross-section values obtained in LHC experiments, along with the extracted parameters, such as, for example, the mass of t quark and the strong coupling constant $\alpha_s(M_Z^2)$, depend crucially on the type of parton distribution functions (PDFs) used in the analyses. Recently, large differences are found in both the cross-section values and the extracted parameters, which were obtained by using Alekhin–Blumlein–Moch (ABM) [2] and Jimenez-Delgado–Reya (JR) PDF sets [3]. The latter were in turn derived mostly by fitting deep inelastic scattering (DIS) data, which is one of the most important processes in studying PDFs in nucleons. Other groups doing such an analysis, namely, CTEQ [4], NN21 Collaborations [5] and MSTW group [6], included in their fits additional experimental data (see a recent review [7] and references therein).

The differences are sometimes seen to be much larger than the individual PDF uncertainties [7, 8] and give rise to mostly different shapes of gluon densities and strong coupling constant $\alpha_s(M_Z^2)$, which are known to be strongly correlated. The values of $\alpha_s(M_Z^2)$ obtained while using the ABM sets [2, 9] are considerably lower than those derived in other

cases and can partially be explained [10] by the usage of the fixed flavor number scheme in the ABM sets.

In the present paper we will focus on the strong coupling constant value. There is another way to decrease the value of $\alpha_s(M_Z^2)$ observed in [2, 9], which is associated with a so-called *BCDMS effect*. The effect comes about upon analyzing stiffly accurate BCDMS data [11], which are very important in fitting the value of $\alpha_s(M_Z^2)$, especially in the analyses based on mostly DIS data, which is the case for ABM sets. However, as it was shown in [12] those precise data were collected with large systematic errors within certain ranges, which can presumably be responsible for an effective decrease in the value of $\alpha_s(M_Z^2)$ (see [1, 12, 13]).

One of the most accurate processes suitable for extracting $\alpha_s(M_Z^2)$ values is the valence part of DIS structure function (SF) F_2 , which is free of any correlations with gluon density. Here we will only consider the valence part¹. The study closely follows similar analyses [1, 13] performed at the next- (NLO) and next-to-next-to-leading-order (NNLO) levels, respectively. The difference between analyses done in [1] and [13] is that only a nonsinglet case is dealt with in the former. In the present paper we consider systematic errors in BCDMS data in a different manner than it was done in [1] in order to study how they influence our results obtained in [1, 13], where $\alpha_s(M_Z^2)$ value was shown to increase when we cut out BCDMS data with the largest systematic errors. Those results have recently been questioned in [9], where it was found that this effect is negligible. The authors of [9] conjectured that the $\alpha_s(M_Z^2)$ value increased due to neglected systematic errors in BCDMS data in the analyses done in [1, 13].

First, we'd like to stress that systematic errors in BCDMS data were not neglected in [1, 13]; moreover, we are going to show that including those BCDMS systematic errors in a different way does not significantly modify our results derived in [1, 13]. Upon omitting the BCDMS data with largest systematic errors we obtain higher values of the coupling constant normalization $\alpha_s(M_Z^2)$ fitted to the experimental data. Moreover, the effect does not strongly depend on specific cut values, as it was observed earlier [1, 13].

BCDMS, SLAC and NMC experimental data on DIS structure function (SF) $F_2(x, Q^2)$ [11, 14, 15] are analyzed at NNLO of massless perturbative QCD. More or less reliable calculations at this level became possible due to $\alpha_s^3(Q^2)$ corrections to the splitting functions (the anomalous dimensions of Wilson operators) [16].

2 Theoretical basis and fitting procedure

As in our previous papers the function $F_2(x, Q^2)$ is represented as a sum of the leading twist $F_2^{pQCD}(x, Q^2)$ and twist four terms

$$F_2(x, Q^2) = F_2^{pQCD}(x, Q^2) \left(1 + \frac{\tilde{h}_4(x)}{Q^2} \right). \quad (1)$$

In the analyses performed over experimental data various effects and corrections must be taken into account. Here the nuclear effects, target mass and heavy quark threshold corrections and higher twist terms are considered. For details we refer to [13, 17].

There in general are two methods of carrying out a QCD analysis over DIS data: the first one (see e.g. [2]-[6]) deals with Dokshitzer-Gribov-Lipatov-Altarelli-Parisi (DGLAP)

¹In the present paper we restrict analysis to the large x region. Consequently, the analysis is dubbed a “valence quark” or “nonsinglet” one (i.e. no gluons take part in the analyses) but actually the data on the total structure function $F_2(x, Q^2)$ will be considered.

integro-differential equations [19] and lets the data be examined directly, whereas the second one involves considering SF moments and therefore allows performing an analysis in the analytic form as opposed to the former. In the present paper we will use an approach that can be thought of as a cross between these two latter, i.e. analysis is carried out over SF moments $F_2^k(x, Q^2)$ defined as follows

$$M_n^{pQCD/twist2/\dots}(Q^2) = \int_0^1 x^{n-2} F_2^{pQCD/twist2/\dots}(x, Q^2) dx \quad (2)$$

followed by the reconstruction of SF for each Q^2 by using a Jacobi polynomial expansion method [20, 21] (for further details see [13, 17]).

Aspects of the analyses related with a Q^2 -evolution of PDF moments (with the analytic continuation [22] in their coefficient functions and anomalous dimensions), PDF normalization, target mass (TMC) and higher twist corrections (HTCs), as well as nuclear effects remain virtually the same as in our previous work [13] so we refer to it for more details.

As usual, the moments $\mathbf{f}_i(n, Q^2)$, ($i = ns, q, g$) at some Q_0^2 is a theoretical input to the analysis. In the fits of data with the cut $x \geq 0.25$ imposed, only the nonsinglet parton density is worked with and the following parametrization at the normalization point is used (see, for example, [1, 23]):

$$\mathbf{f}(n, Q^2) = \int_0^1 dx x^{n-2} \tilde{\mathbf{f}}(x, Q^2), \quad \tilde{\mathbf{f}}(x, Q^2) = A(Q^2) x^{\lambda(Q^2)} [1-x]^{b(Q^2)} [1+d(Q^2)x], \quad (3)$$

where $A(Q^2)$, $\lambda(Q^2)$, $b(Q^2)$ and $d(Q^2)$ are some coefficient functions.

Recall also some salient points of the so-called polynomial expansion method. The latter was first proposed in [24] and further developed in [25]. The Jacobi polynomials were first proposed and subsequently developed in [20, 21] with the purpose of analyzing the experimental data on SFs. They were then extensively used in [23]-[29].

With the QCD expressions for the Mellin moments $M_n^k(Q^2)$ (see, for example, [17]) the SF $F_2^k(x, Q^2)$ is reconstructed by using the Jacobi polynomial expansion method:

$$F_2^k(x, Q^2) = x^a (1-x)^b \sum_{n=0}^{N_{max}} \Theta_n^{a,b}(x) \sum_{j=0}^n c_j^{(n)}(\alpha, \beta) M_{j+2}^k(Q^2),$$

where $\Theta_n^{a,b}$ are the Jacobi polynomials and a, b are the parameters to be fitted. A condition put on the latter is the requirement of the error minimization while reconstructing the structure functions. MINUIT package [30] is used to minimize two variables; namely, the function F_2 itself and its logarithmic ‘‘slope’’ $d \ln F_2(x, Q^2) / d \ln \ln(Q^2/\Lambda^2)$. The twist expansion is thought to be applicable above approximately $Q^2 \sim 1 \text{ GeV}^2$ hence the global cut $Q^2 \geq 1 \text{ GeV}^2$ imposed upon the data throughout.

The systematic errors for BCDMS data are given [11] as multiplicative factors to the experimental $F_2(x, Q^2)$ value. Denoted as f_r, f_b, f_s, f_d and f_h they are in fact uncertainties caused by the spectrometer resolution, beam momentum, calibration, spectrometer magnetic field calibration, detector inefficiencies and the energy normalization, respectively. In the previous paper [1] the experimental value in each point of the original dataset was multiplied by the factor characterizing the type of uncertainties, one at a time, and thus modified dataset for the analyzed quantity was then fitted by using the procedure sketched above. Afterwards, all the systematic errors obtained this way were taken together in quadrature to yield the total one. In the present paper, instead of using that multiplicative approach, the total systematic error for α_s is obtained by taking into

account all those five uncertainties in quadrature at each experimental point and then used to calculate the total experimental error.

We use free normalizations of the data for different experiments. For a reference set, the most stable deuterium BCDMS data at the value of the beam initial energy $E_0 = 200$ GeV is used. When other datasets are taken as a reference one, variation in the results is found to be negligible. In the case of the fixed normalization for each and all datasets the fits tend to yield a little bit worse χ^2 , just as was observed earlier.

3 Results

As is known a nonsinglet analysis features no gluons taking part in the analysis; therefore, the cut imposed over the Bjorken variable ($x \geq 0.25$) effectively excludes the region where gluon density is believed to be non-negligible.

A starting point of the evolution is $Q_0^2 = 90$ GeV² for BCDMS and all datasets, and $Q_0^2 = 20$ GeV² — for combined SLAC and NMC datasets. These Q_0^2 values are close to the average values of Q^2 spanning the corresponding data. The heavy quark thresholds are taken at $Q_f^2 = m_f^2$. Following our previous papers the maximum number of moments to be accounted for in the analyses is taken to be $N_{max} = 8$ [21] and the additional cut $x \leq 0.8$ is imposed everywhere.

3.1 α_s from individual BCDMS and SLAC+NMC analyses

Analysis starts with the most precise experimental data [11] obtained by the BCDMS muon scattering experiment for large Q^2 values. A complete set of data includes 607 points when the cut $x \geq 0.25$ is imposed. An original analysis carried out by the BCDMS collaboration (see also [18]) gave (back then) comparatively small values for the strong coupling constant; for example, $\alpha_s(M_Z^2) = 0.113$ at NLO was quoted in the latter reference.

Much like in [1, 13] the data with largest systematic errors are cut out by imposing certain limits on the kinematic variable $Y = (E_0 - E)/E_0$ (where E_0 and E are lepton's initial and final energies, respectively [12]). The following y cuts depending on the limits put on x are imposed:

$$\begin{aligned}
 y &\geq 0.14 && \text{for } 0.3 < x \leq 0.4 \\
 y &\geq 0.16 && \text{for } 0.4 < x \leq 0.5 \\
 y &\geq Y_{cut3} && \text{for } 0.5 < x \leq 0.6 \\
 y &\geq Y_{cut4} && \text{for } 0.6 < x \leq 0.7 \\
 y &\geq Y_{cut5} && \text{for } 0.7 < x \leq 0.8
 \end{aligned}$$

An impact of experimental systematic errors on the results of QCD analysis is studied for a few sets of Y_{cut3} , Y_{cut4} and Y_{cut5} cuts given in Table 1.

Table 1. A set of Y_{cut3} , Y_{cut4} and Y_{cut5} values used in the analysis ²

$N_{Y_{cut}}$	1	2	3	4	5
Y_{cut3}	0.16	0.16	0.18	0.22	0.23
Y_{cut4}	0.18	0.20	0.20	0.23	0.24
Y_{cut5}	0.20	0.22	0.22	0.24	0.25

Following the analyses performed in [1, 13], we arrive at similar results: α_s values for both original and modified (by cuts) datasets are shown in Tables 2 and 3, where a total systematic error is estimated in quadrature by using the method somewhat different from that utilized in our earlier analyses. ($N_{Y_{cut}} = 0$ corresponds to the case without Y cuts). Namely, instead of accounting for those errors by the multiplication procedure (an old approach outlined in [1]), here they are taken altogether in quadrature from the very beginning.

Table 2. NLO $\alpha_s(M_Z^2)$ values for various sets of Y cuts

$N_{Y_{cut}}$	number of points	χ^2 quad. syst. err. (mult. syst. err.)	$\alpha_s(M_Z^2)$ \pm stat. error quad. syst. err.	$\alpha_s(M_Z^2)$ \pm stat. error mult. syst. err.	total syst. error
0	607	444 (609)	0.1078 ± 0.0012	0.1072 ± 0.0012	0.0054
1	502	358 (477)	0.1149 ± 0.0015	0.1146 ± 0.0015	0.0039
2	495	355 (469)	0.1151 ± 0.0015	0.1148 ± 0.0015	0.0038
3	489	350 (459)	0.157 ± 0.0015	0.1155 ± 0.0015	0.0036
4	458	327 (423)	0.1166 ± 0.0016	0.1163 ± 0.0016	0.0031
5	452	322 (417)	0.1172 ± 0.0016	0.1168 ± 0.0016	0.0030

Table 3. NNLO $\alpha_s(M_Z^2)$ values for various sets of Y cuts

$N_{Y_{cut}}$	number of points	χ^2 quad. syst. err. (mult. syst. err.)	$\alpha_s(M_Z^2)$ \pm stat. error quad. syst. err.	$\alpha_s(M_Z^2)$ \pm stat. error mult. syst. err.	total syst. error
0	607	446 (642)	0.1064 ± 0.0012	0.1056 ± 0.0012	0.0054
1	502	361 (481)	0.1132 ± 0.0015	0.1127 ± 0.0015	0.0039
2	495	357 (477)	0.1135 ± 0.0015	0.1130 ± 0.0015	0.0038
3	489	352 (463)	0.1140 ± 0.0015	0.1136 ± 0.0015	0.0036
4	458	350 (427)	0.1150 ± 0.0016	0.1144 ± 0.0016	0.0031
5	452	325 (421)	0.1155 ± 0.0016	0.1149 ± 0.0016	0.0030

Once the cuts are imposed (in what follows we work with a set $N_{Y_{cut}} = 5$), only 452 points left available for analysis. Fitting them according to the procedure outlined above the following results are obtained:

$$\alpha_s(M_Z^2) = 0.1155 + \left\{ \begin{array}{l} \pm 0.0016 \text{ (stat)} \pm 0.0030 \text{ (syst)} \pm 0.0007 \text{ (norm)} \\ \pm 0.0035 \text{ (total exp. error)} \end{array} \right. , \quad (4)$$

²This set slightly differs from that presented in [1, 13].

where an abbreviation “norm” denotes the experimental data normalization error stemming from the difference of the fits with free and fixed normalizations of BCDMS data subsets [11] featuring different beam energy values.

In view of a few NMC data points in the region $x \geq 0.25$, we have performed similar combined fits of SLAC and NMC datasets and found the following NNLO result for the strong coupling normalization (which is obtained under the same conditions as the one presented in the last row of Table IV in [1]):

$$\alpha_s(M_Z^2) = 0.1180 + \begin{cases} \pm 0.0014 \text{ (stat)} \pm 0.0036 \text{ (syst)} \pm 0.0008 \text{ (norm)} \\ \pm 0.0039 \text{ (total exp. error)}. \end{cases} \quad (5)$$

3.2 α_s and HTC parameters in combined SLAC, BCDMS and NMC analysis

As in the case of BCDMS data analysis the cuts imposed are $x \geq 0.25$ and $N_{Y_{cut}} = 5$ (see Table 1). Then, an overall set of data consists of 756 points.

In order to determine the region where perturbative QCD is applicable we start by analyzing the data without a contribution of twist-four terms (that is $F_2 = F_2^{pQCD}$) and perform several fits with the cut $Q^2 \geq Q_{min}^2$ gradually increased. Table 4 demonstrates that the quality of fits appears to be already acceptable beginning from $Q^2 = 2 \text{ GeV}^2$.

Now, the twist-four corrections are added and the data with a global cut $Q^2 \geq 1 \text{ GeV}^2$ is fitted. As in the previous studies [1, 13] it is clearly seen that higher twists improve the fit quality, with an insignificant discrepancy in the values of the coupling constant to be quoted below.

Table 4. $\alpha_s(M_Z^2)$ and χ^2 in the combined SLAC, BCDMS, NMC analysis

Q_{min}^2	N of points	HTC	$\chi^2(F_2)/\text{DOF}$	$\alpha_s(90 \text{ GeV}^2) \pm \text{stat}$	$\alpha_s(M_Z^2)$
1.0	756	No	1.41	0.1757 ± 0.0007	0.1160
2.0	731	No	1.03	0.1758 ± 0.0007	0.1161
3.0	704	No	0.84	0.1787 ± 0.0009	0.1173
4.0	682	No	0.79	0.1790 ± 0.0009	0.1174
5.0	662	No	0.79	0.1795 ± 0.0011	0.1177
6.0	637	No	0.79	0.1798 ± 0.0013	0.1178
7.0	610	No	0.78	0.1792 ± 0.0016	0.1175
8.0	594	No	0.79	0.1787 ± 0.0019	0.1173
9.0	575	No	0.78	0.1785 ± 0.0023	0.1172
10.0	564	No	0.77	0.1765 ± 0.0026	0.1164
1.0	756	Yes	0.88	0.1750 ± 0.0019	0.1157

The following values for PDF parametrization parameters are obtained in the fit corresponding to the last row of the above table (errors shown are actually the symmetric ones):

$$\begin{aligned} A(H_2) &= 3.443 \pm 0.046, & A(D_2) &= 9.201 \pm 0.111, & A(C) &= 7.580 \pm 0.173, \\ \lambda(H_2) &= 0.143 \pm 0.007, & \lambda(D_2) &= 0.494 \pm 0.007, & \lambda(C) &= 0.340 \pm 0.015, \\ b(H_2) &= 4.144 \pm 0.013, & b(D_2) &= 3.795 \pm 0.019, & b(C) &= 3.615 \pm 0.036, \\ d(H_2) &= 3.223 \pm 0.072, & d(D_2) &= -0.404 \pm 0.024, & d(C) &= -0.629 \pm 0.034. \end{aligned}$$

They are seen to be very similar to those presented in [1].

Twist-four parameter values are presented in Table 5. Note that these for H_2 and D_2 targets are obtained in separate fits by analyzing SLAC, NMC and BCDMS datasets altogether.

Table 5. Parameter values of the twist-four term in different orders

x	LO \pm stat		NLO \pm stat		NNLO \pm stat	
	$h_4(x)$ for H_2	$h_4(x)$ for D_2	$h_4(x)$ for H_2	$h_4(x)$ for D_2	$h_4(x)$ for H_2	$h_4(x)$ for D_2
0.275	-0.275 ± 0.012	-0.274 ± 0.021	-0.251 ± 0.026	-0.221 ± 0.007	-0.176 ± 0.023	-0.136 ± 0.026
0.35	-0.269 ± 0.015	-0.246 ± 0.030	-0.190 ± 0.025	-0.178 ± 0.006	-0.143 ± 0.032	-0.021 ± 0.015
0.45	-0.181 ± 0.016	-0.125 ± 0.049	-0.290 ± 0.017	-0.002 ± 0.010	-0.181 ± 0.031	-0.068 ± 0.015
0.55	-0.049 ± 0.033	0.080 ± 0.082	-0.316 ± 0.031	0.247 ± 0.014	-0.233 ± 0.059	0.043 ± 0.022
0.65	0.326 ± 0.063	0.357 ± 0.144	-0.064 ± 0.076	0.563 ± 0.035	-0.167 ± 0.156	0.353 ± 0.059
0.75	0.805 ± 0.124	0.513 ± 0.213	0.009 ± 0.122	0.770 ± 0.070	-0.156 ± 0.215	0.323 ± 0.104

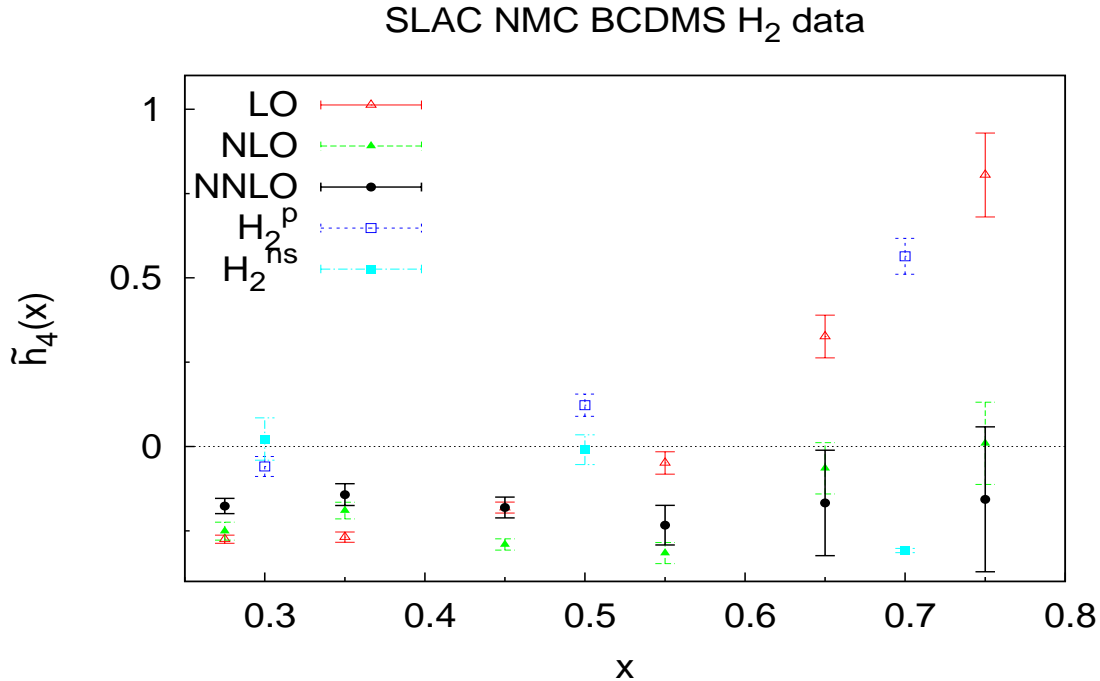


Figure 1: Twist-four $\tilde{h}_4(x)$ parameter values obtained at LO, NLO and NNLO for hydrogen data (bars show statistical errors). For comparison, H_2^p and H_2^{ns} points borrowed from [2] are also shown.

HTCs are shown in Figs. 1 and 2, where twist-four corrections obtained at NLO and NNLO are observed to be compatible with each other. Their values in Table 5 are very similar to those presented in [1]. Therefore, all the comments in [1] can be applied also to the present case and we won't be repeating discussions given there. We would only like to stress that the cut imposed on BCDMS data, which effectively increased α_s values (see Tables 2 and 3), essentially improves also an agreement between theory and experiment. HTCs as being the difference between the twist-two approximation (i.e. pure perturbative QCD contribution) and the experimental data becomes considerably smaller at NLO and NNLO levels compared with NLO HT terms obtained in [18] and also with the results of analysis with no Y -cuts imposed over BCDMS data (see Figs. 5, 6 in [1]).

SLAC NMC BCDMS D_2 data

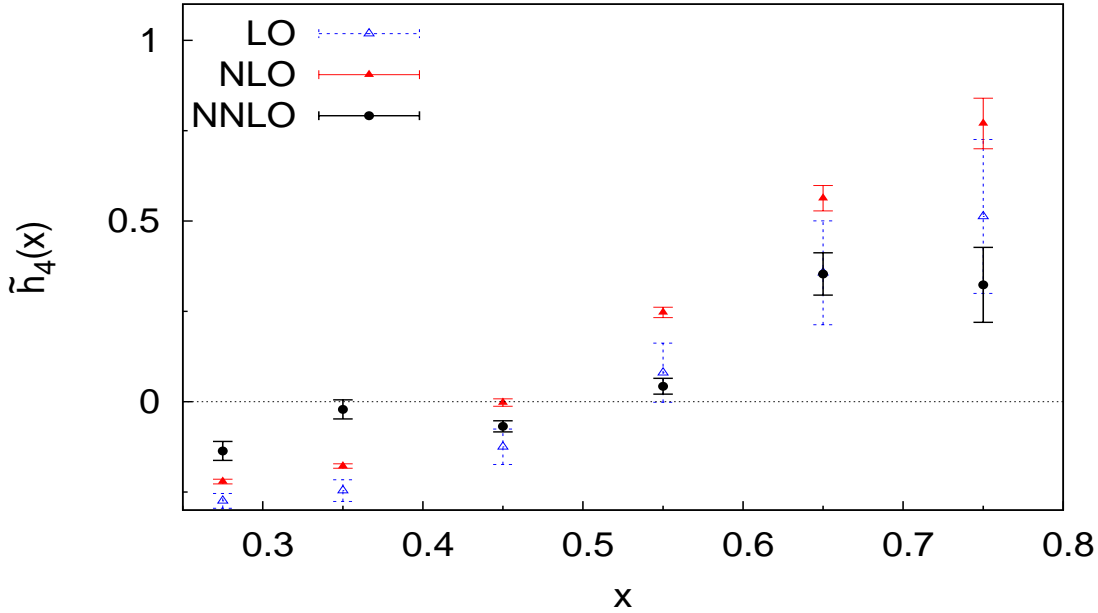


Figure 2: The same as in Fig. 1 for deuterium data.

Some additional support of these observations can be gained by considering NNLO HTCs presented in [9], which are shown ³ in Fig. 1. HTCs obtained in [9] are seen to be virtually higher than our ones. However, they are well compatible with the corresponding HTCs, obtained in the analysis with no Y -cuts imposed over BCDMS data (see Fig. 5 in [1]).

Figure 1 also displays HTC results for the nonsinglet part of F_2 borrowed from [9]. They demonstrate the difference in the HTC shapes for H_2 and D_2 cases, which agrees with our results presented in Table 5 and Figs. 1 and 2.

In order to assess the quality of fits we present the correlation matrix of the fit parameters (Appendix A) and pulls for individual datasets (Appendix B).

Finally, using the nonsinglet evolution analyses of SLAC, NMC and BCDMS experimental data for SF F_2 with no account for twist-four corrections and the cut $Q^2 \geq 2$ GeV², we obtain (with $\chi^2/DOF = 1.03$)

$$\alpha_s(M_Z^2) = 0.1161 + \begin{cases} \pm 0.0003 \text{ (stat)} \pm 0.0018 \text{ (syst)} \pm 0.0007 \text{ (norm)} \\ \pm 0.0020 \text{ (total exp.error)} \end{cases} . \quad (6)$$

Upon including the twist-four corrections, and imposing the cut $Q^2 \geq 1$ GeV², the following result is found (with $\chi^2/DOF = 0.88$):

$$\alpha_s(M_Z^2) = 0.1157 + \begin{cases} \pm 0.0008 \text{ (stat)} \pm 0.0020 \text{ (syst)} \pm 0.0005 \text{ (norm)} \\ \pm 0.0022 \text{ (total exp.error)} \end{cases} . \quad (7)$$

Results for $n = 2$ moment of the difference of valence parts of the u and d quarks are also investigated in the lattice models. Following [28, 9], we will try to estimate this second moment.

³The authors of [9] used another HTC definition. Upon translating the latter to our definition it looks like $F_2(x, Q^2) = F_2^{QCD}(x, Q^2) + \tilde{H}_4(x)/Q^2$. So, the functions $\tilde{h}_4(x)$ can be estimated in the following way: $\tilde{h}_4(x) = \tilde{H}_4(x)/F_2^{QCD}(x, Q^2)$, where we can use $Q^2 = 2.5$ GeV², which is a lower Q^2 boundary in the analysis [9].

They can be extracted at large x values directly from the difference of the nonsinglet parton densities in proton and deuteron:

$$\tilde{\mathbf{f}}_u^v(x, Q^2) - \tilde{\mathbf{f}}_d^v(x, Q^2) \approx \tilde{\mathbf{f}}_p(x, Q^2) - \tilde{\mathbf{f}}_d(x, Q^2), \quad (8)$$

because in this case the contribution of sea quarks and antiquarks is negligible (see, for example, recent papers [31]).

This way, by using the results given in Eq. (6) we obtain the difference of second moments $\mathbf{f}_u^v(2, Q^2) - \mathbf{f}_d^v(2, Q^2)$, shown in Table 6.

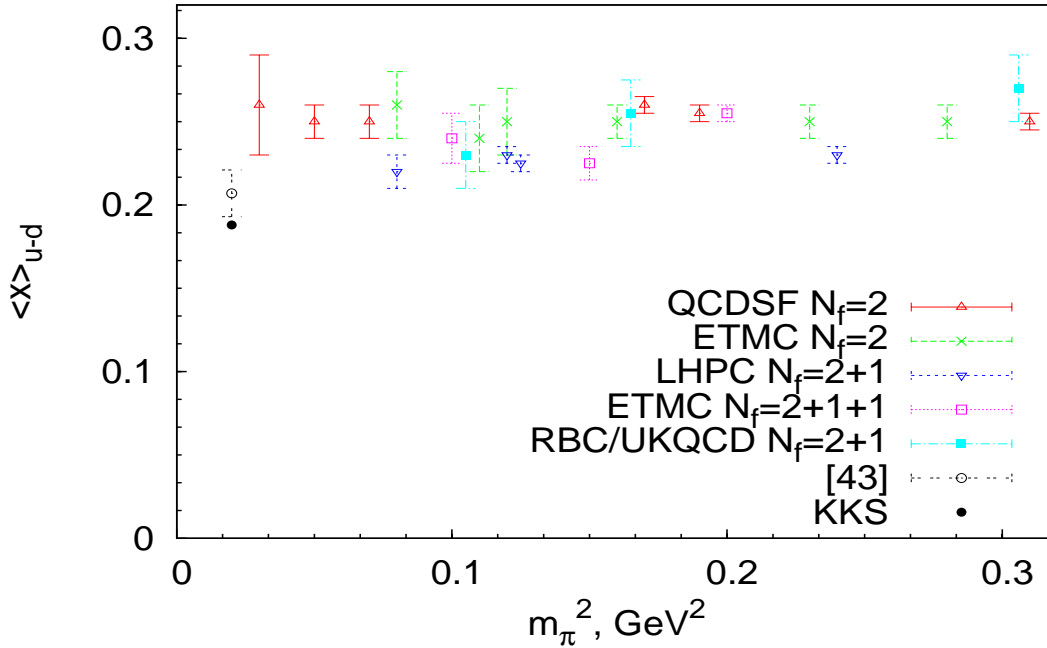


Figure 3: Results of lattice computations for the second moment of non-singlet density as a function of the pion mass m_π . Our result (KKS) for $\langle x \rangle_{u-d} \equiv \mathbf{f}_u^v(2, Q^2) - \mathbf{f}_d^v(2, Q^2)$ is given for $Q^2 = 1 \text{ GeV}^2$.

Table 6. Results for the difference $\mathbf{f}_u^v(2, Q^2) - \mathbf{f}_d^v(2, Q^2)$.

$Q^2, \text{ GeV}^2$	90	4	2	1
diff.	0.115 ± 0.053	0.146 ± 0.067	0.157 ± 0.073	0.188 ± 0.087

As seen from Table 6, at $Q^2 = 4 \text{ GeV}^2$ the difference derived in the present paper is approximately 10 ÷ 15% less than that quoted in [9, 28]. Note that the lattice results are strongly nonperturbative; it would therefore be better to compare them with our result obtained at $Q^2 = 1 \text{ GeV}^2$, which corresponds in the analysis under consideration to the boundary between perturbative and nonperturbative QCD. This comparison with the respective lattice results is presented in Fig. 3. Being a difference of two large quantities it has a large error and therefore only a central value of $\langle x \rangle_{u-d}$ is shown in the figure.

The lattice points except for the leftmost one are taken from the lattice collaborations: QCDSF ($n_f = 2$) [32], RBC/UKQCD ($n_f = 2 + 1$) [33], LHPC ($n_f = 2 + 1$) [34], ETMC ($n_f = 2$) [35], ETMC ($n_f = 2 + 1$) [36, 37]. The leftmost point is borrowed from the recent paper [38]. As seen in Fig. 3, it agrees well with our result for $\mathbf{f}_u^v(2, Q^2) - \mathbf{f}_d^v(2, Q^2)$ obtained at $Q^2 = 1 \text{ GeV}^2$. Note that the result similar to those published in [38], have recently been obtained in [39] (see review in [40]).

4 Scale dependence

In this section the dependence of the results on the different choice of the factorization $\mu_F = k_F Q^2$ and renormalization $\mu_R = k_R Q^2$ scales is studied. The threshold crossing point is taken at $Q_f^2 = m_f^2$. Following [18] we choose three values (1/2, 1, 2) for the coefficients k_F and k_R .

Results are demonstrated in Table 7. Fits are performed with no account for higher twist corrections, the number of points is 731 (SLAC, BCDMS and NMC data), $Q_{min}^2 = 2$ GeV² and different datasets are freely normalized. The change in $\alpha_s(M_Z^2)$ value for various k_F and k_R values is denoted by the difference:

$$\Delta\alpha_s(M_Z^2) = \alpha_s(M_Z^2) - \alpha_s(M_Z^2)|_{k_F=k_R=1} \quad (9)$$

Table 7. $\alpha_s(M_Z^2)$ for a set of k_F and k_R coefficients

k_R	k_F	$\chi^2(F_2)$	$\alpha_s(90 \text{ GeV}^2) \pm \text{stat}$	$\alpha_s(M_Z^2)$	$\Delta\alpha_s(M_Z^2)$
1	1	712	0.1758 ± 0.0007	0.1161	0
1/2	1	660	0.1729 ± 0.0007	0.1149	-0.0012
1	1/2	587	0.1733 ± 0.0006	0.1150	-0.0011
1	2	852	0.1808 ± 0.0008	0.1182	+0.0021
2	1	785	0.1805 ± 0.0008	0.1180	+0.0019

As seen from this table theoretical uncertainties for the maximum and minimum values of the coupling constant corresponding to $k_i = 2$ and $k_i = 1/2$ ($i = F, R$), respectively, are found to be +0.0028 and -0.0016.⁴ It should be noted that we take into account renormalization scale uncertainty in the expressions for the coefficient functions and respective coupling constants analogously to what was done in [41].

Thus, NS evolution analyses of SLAC, NMC and BCDMS experimental data for SF F_2 give for $\alpha_s(M_Z^2)$ the following numbers (with no account for HTC, $Q^2 \geq 2$ GeV² and $\chi^2 = 1.03$):

$$\alpha_s(M_Z^2) = 0.1161 + \left\{ \begin{array}{l} \pm 0.0003 \text{ (stat)} \pm 0.0018 \text{ (syst)} \pm 0.0007 \text{ (norm)} \\ \pm 0.0020 \text{ (total exp.error)} \end{array} \right\} + \left\{ \begin{array}{l} +0.0028 \\ -0.0016 \end{array} \right\} \text{ (theor)}.$$

5 Conclusions

In this work the Jacobi polynomial expansion method developed in [20, 21] was used to analyze Q^2 -evolution of DIS structure function F_2 by fitting reliable fixed-target experimental data that satisfy the cut $x \geq 0.25$. Based on the results of fitting, the strong coupling constant value is evaluated at the normalization point. Starting with the reanalysis of BCDMS data by cutting off the points with largest systematic errors it is shown that as earlier $\alpha_s(M_Z^2)$ values rise sharply with the cuts on systematics imposed. On the other hand, the latter do not depend on a certain cut within statistical errors. The present

⁴ Note that here we take theoretical errors for the factorization and renormalization scales in quadrature. In our previous analyses [1, 13] we considered the cases with $k_F = k_R = 1/2$ and $k_F = k_R = 2$ that corresponded to taking the scales together linearly rather than in quadrature.

results are compatible with those obtained in our earlier paper [1], where systematic errors in BCDMS data were taken into account in a different way. To be more precise, in [1], and in even earlier studies [21, 13], systematics was dealt with as follows: all fits were done with experimental data multiplied by respective systematical errors for F_2 separately for each source of uncertainties. Then, the differences between fits with different sources taken into account give rise to the total systematic error derived in quadrature. In the present paper, BCDMS systematics is dealt with in a quadrature rather than in a multiplicative manner right from the start.

Taking into account systematic errors in BCDMS data does not change results of the fits obtained in [1] except for just a single detail: now perturbative QCD (without HTC) is well compatible with the experimental data already at $Q^2 \geq 2 \text{ GeV}^2$ (see Table 4).

Here we would like to give some explanations of no-rise effect in $\alpha_s(M_Z^2)$ value upon cutting out the regions in BCDMS data with larger systematic errors stated in [9]. Note that the values of systematic errors are rather large in the cut out regions but not infinitely large. In the latter case there of course is no any effect of absence/existence of the cut out regions. One of possible explanations relates with the fact that Ref. [9] includes combined singlet and nonsinglet analyses, where there is some correlation between $\alpha_s(M_Z^2)$ values and the shape of gluon density. So, cutting out BCDMS data with the largest systematic errors could lead in [9] to the shape of gluon density somewhat altered.

It turns out that for $Q^2 \geq 2 \text{ GeV}^2$ the formulæ of pure perturbative QCD (i.e. twist-two approximation along with the target mass corrections) are enough to achieve good agreement with all the data analyzed. The reference result is then found to be

$$\alpha_s(M_Z^2) = 0.1161 \pm 0.0020 \text{ (total exp.error)}, \quad (10)$$

Upon adding twist-four corrections, fairly good agreement between QCD and the data starting already at $Q^2 = 1 \text{ GeV}^2$, where the Wilson expansion starts to be applicable, is observed. This way we obtain for the coupling constant at Z mass peak:

$$\alpha_s(M_Z^2) = 0.1157 \pm 0.0022 \text{ (total exp.error)}. \quad (11)$$

Note that in a sense, our results are between those obtained in [9, 2] and [3] (a dynamical approach) and, respectively, results derived by MSTW [6] and NN21 [5] groups. They are consistent with those obtained in [4], [3] (a standard fit) and also with studies of the recent data of CMS and ATLAS collaborations done in [42] and [43], respectively (see the recent review [44]). A complete agreement with recent results obtained in lattice QCD [45] is also observed. There also is very good agreement with lattice QCD results for the second moment $\langle x \rangle_{u-d}$ (see Fig. 3). Our result is slightly below the central world average value

$$\alpha_s(M_Z^2)|_{\text{world average}} = 0.1185 \pm 0.0006, \quad (12)$$

presented in [46], but still compatible within errors.

As was already pointed out the values of theoretical uncertainties, given by this dependence of the results for $\alpha_s(M_Z^2)$ are equal to

$$\Delta\alpha_s(M_Z^2)|_{\text{theor}} = \begin{cases} +0.0028 \\ -0.0016 \end{cases}. \quad (13)$$

It is seen that the theoretical uncertainties are already comparable with the total experimental error. Nonetheless, further account of even higher corrections is still desirable and the next step is to consider further corrections (i.e. those coming from three loops) in the coefficient functions [47], which allows performing N³LO fits at large x values, where

the contributions of the corresponding four-loop corrections to yet unknown anomalous dimensions should be negligible. Note that several N³LO fits had already been done in [27, 28].

The results obtained in the present paper might be useful in shedding some extra light on the differences in the predictions for observables at the LHC found recently [7, 8], which are resulted from the utilization of different sets of parton distribution functions obtained by different groups. Indeed, excluding the ranges with largest systematic errors in BCDMS data increases the value of $\alpha_s(M_Z^2)$ in the fits based on mostly DIS experimental data and could therefore potentially lead to those differences somewhat reduced.

In order to check whether there is effect of the rise in $\alpha_s(M_Z^2)$ value when y -cuts are imposed, it is needed to consider combined nonsinglet and singlet analysis of DIS experimental data over an entire x region. An application of some resummations, like a Grunberg’s effective charge method [48] (as it was done in [29] at the NLO approximation) and the “frozen” (see [49] and references therein) and analytic [50] versions of the strong coupling constant (see [49, 51, 52] for recent studies in this direction) could also be useful in understanding the subject. These are left for the future investigations.

6 Acknowledgments

The work was supported by RFBR grant No.13-02-01005-a.

7 Appendix A

Here we present a correlation matrix of the fit parameters derived in the case shown in the last row of Table 4. As it is seen, there are non-negligible correlations between carbon A, b, d and hydrogen d and deuterium A, d parameters, while no appreciable correlations are observed for the strong coupling and Jacobi parameters. By varying fit parameters and their limits we have verified that the final results are not significantly affected by these correlations, though the latter were more or less persistent.

Table 8. *Correlation matrix of the parameters for the combined fit with HTC*

	A_{H_2}	b_{H_2}	d_{H_2}	A_{D_2}	b_{D_2}	d_{D_2}	$\alpha_s(Q_0^2)$	A_C	b_C	d_C	b	a
A_{H_2}	1.000											
b_{H_2}	0.271	1.000										
d_{H_2}	-0.721	0.298	1.000									
A_{D_2}	-0.593	0.303	0.873	1.000								
b_{D_2}	0.734	0.011	-0.743	-0.491	1.000							
d_{D_2}	0.719	-0.304	-0.963	-0.893	0.734	1.000						
$\alpha_s(Q_0^2)$	0.019	-0.278	-0.387	-0.544	-0.017	0.339	1.000					
A_C	0.672	-0.306	-0.921	-0.917	0.670	0.955	0.359	1.000				
b_C	-0.727	0.249	0.955	0.896	-0.716	-0.961	-0.407	-0.891	1.000			
d_C	-0.716	0.290	0.964	0.936	-0.710	-0.987	-0.396	-0.972	0.967	1.000		
b	0.164	0.369	-0.027	0.131	0.209	0.003	0.144	0.006	0.045	0.017	1.000	
a	-0.347	-0.147	0.193	0.000	-0.477	-0.202	0.552	-0.165	0.164	0.167	0.286	1.000

8 Appendix B. Pulls for the individual datasets

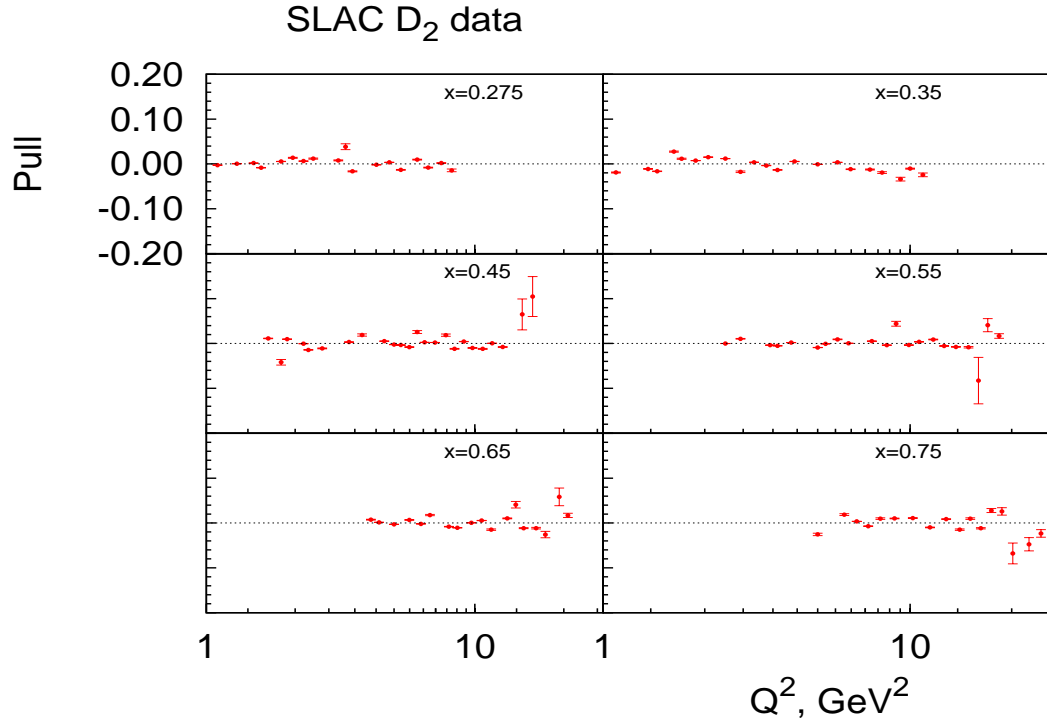


Figure 4: Pulls obtained in NNLO QCD analysis of SLAC deuterium data (bars include statistical and systematic uncertainties).

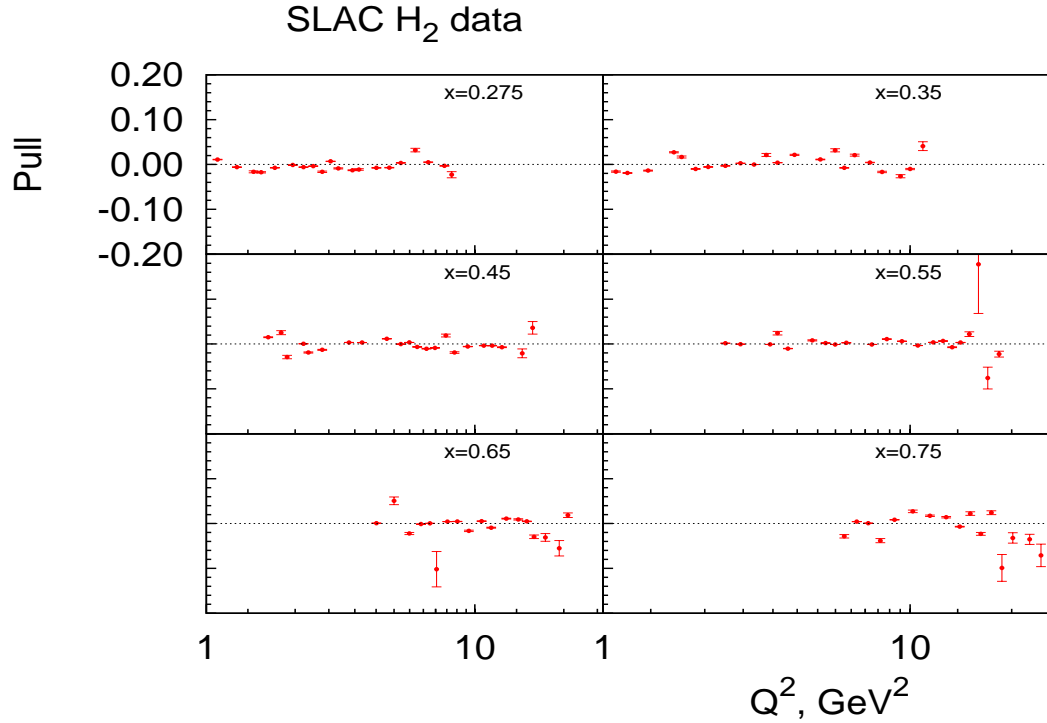


Figure 5: The same as in Fig. 1 for SLAC hydrogen data.

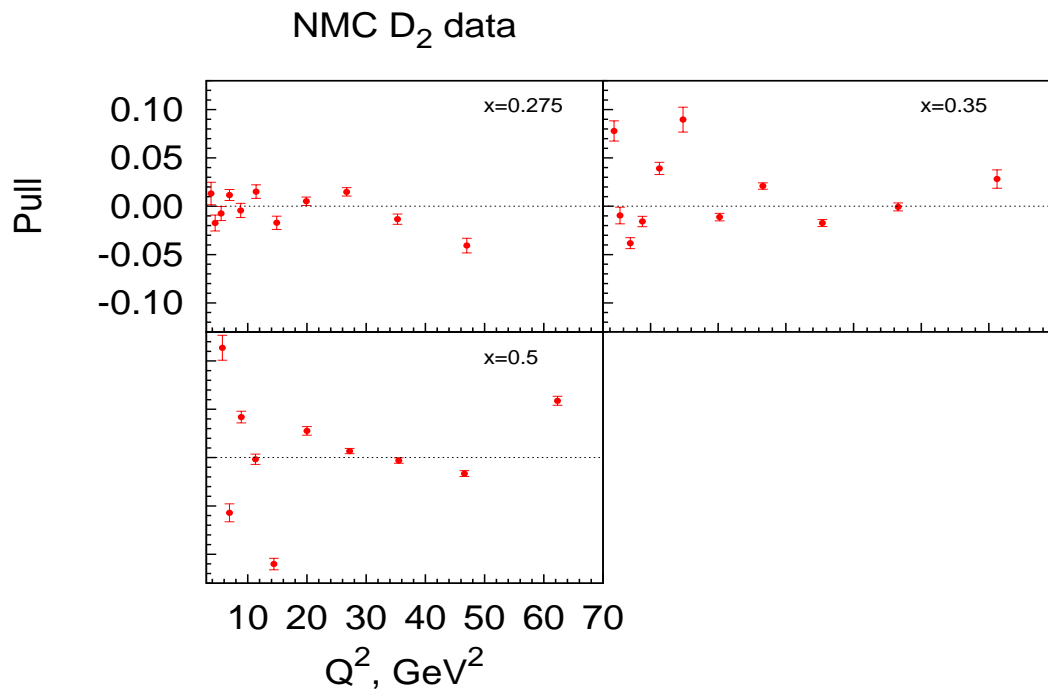


Figure 6: The same as in Fig. 1 for NMC deuterium data.

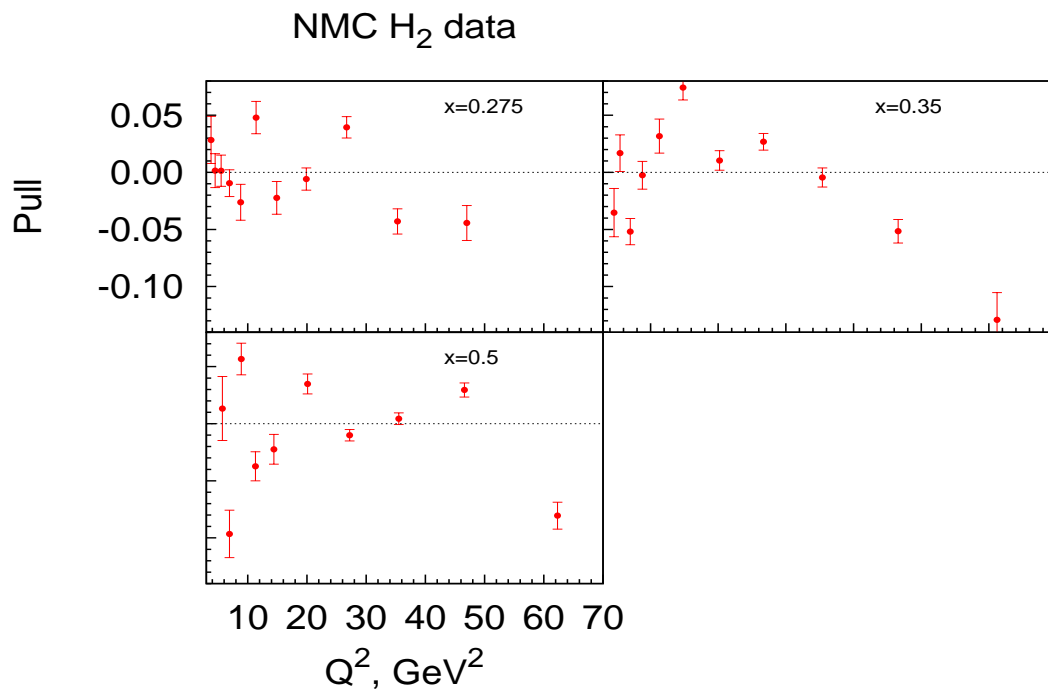


Figure 7: The same as in Fig. 1 for NMC hydrogen data.

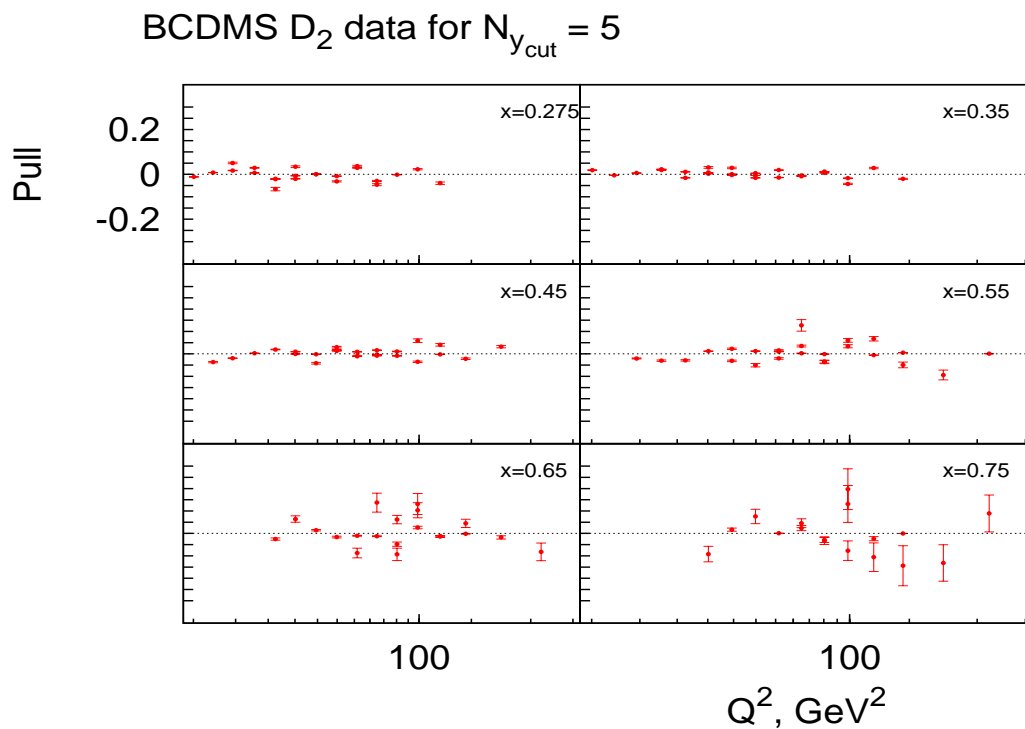


Figure 8: The same as in Fig. 1 for BCDMS deuterium data.

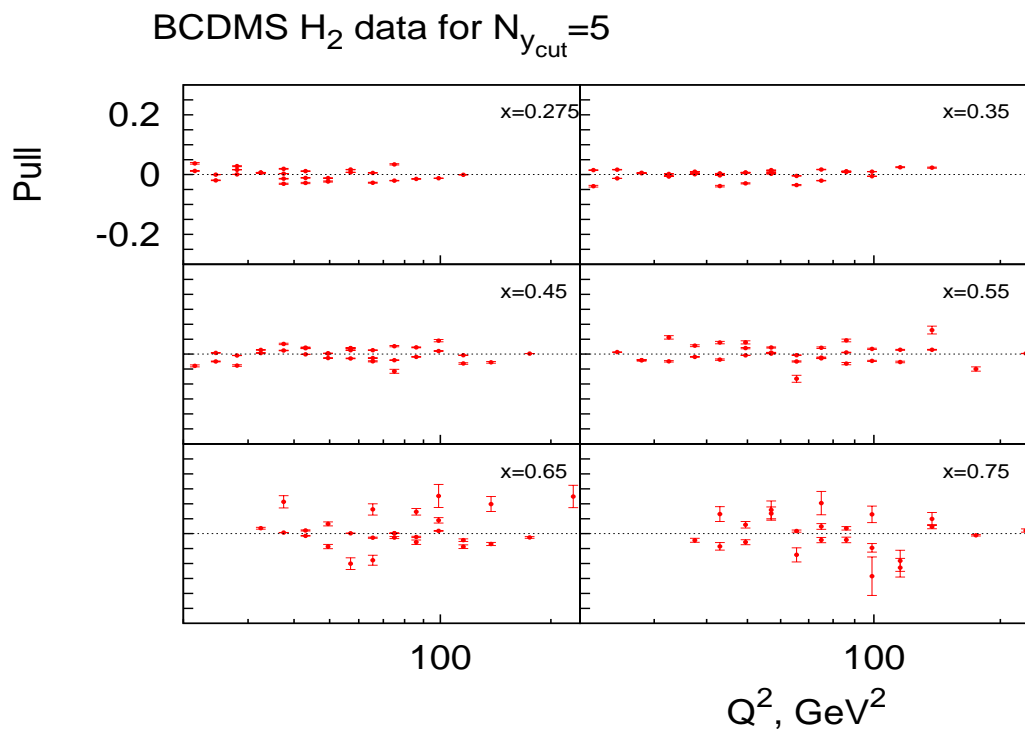


Figure 9: The same as in Fig. 1 for BCDMS hydrogen data.

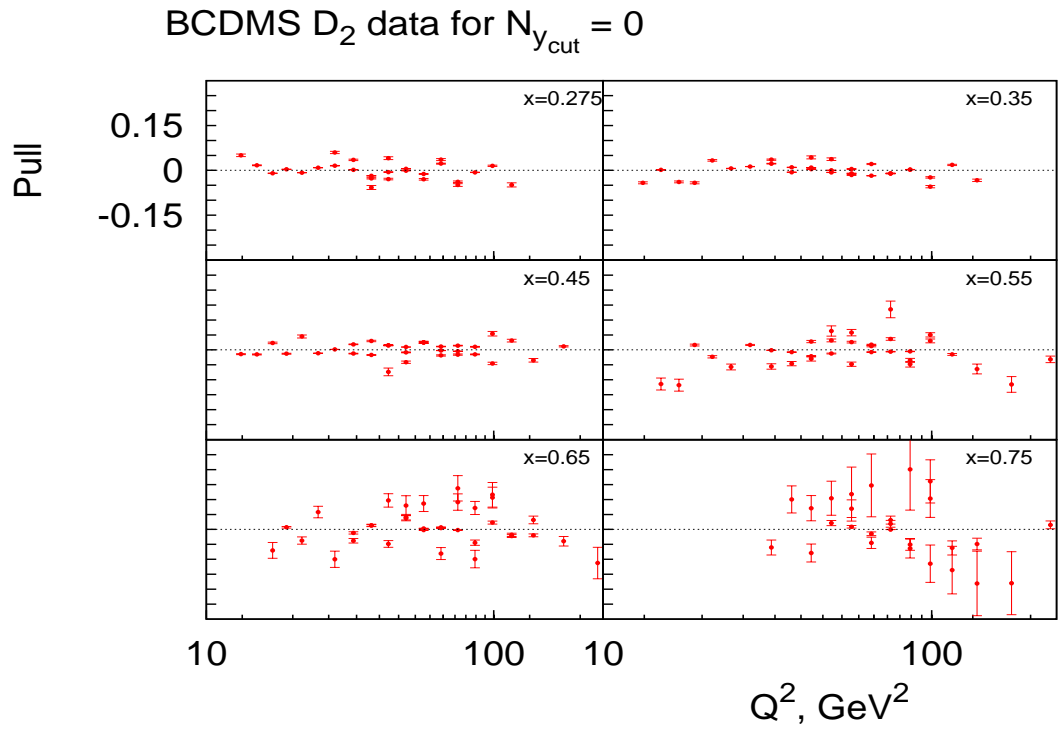


Figure 10: The same as in Fig. 1 for BCDMS deuterium data before y cuts are imposed.

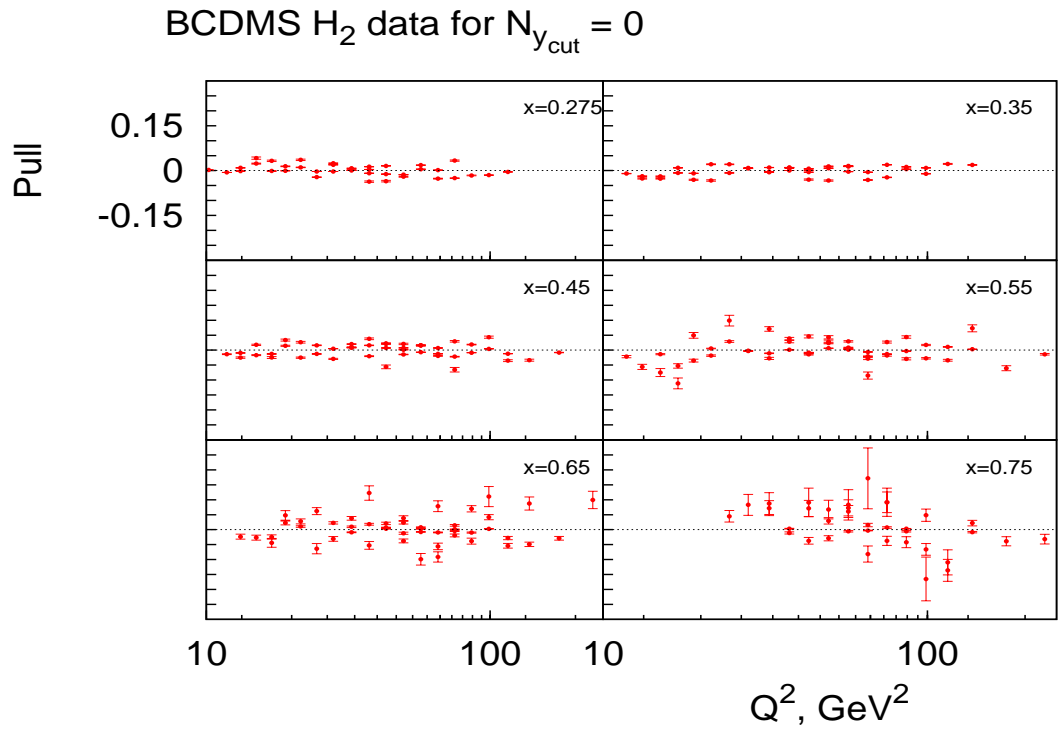


Figure 11: The same as in Fig. 1 for BCDMS hydrogen data before y cuts are imposed.

References

- [1] B. G. Shaikhatdenov, A. V. Kotikov, V. G. Krivokhizhin and G. Parente, Phys. Rev. **D 81** (2010) 034008 [Erratum-ibid. **D 81** (2010) 079904]
- [2] S. Alekhin, J. Bluemlein and S. Moch, Phys. Rev. **D 89** (2014) 054028.
- [3] P. Jimenez-Delgado and E. Reya, Phys. Rev. **D 79** (2009) 074023; Phys. Rev. **D 89** (2014) 074049.
- [4] J. Gao *et al.*, Phys. Rev. **D 89** (2014) 3, 033009.
- [5] R. D. Ball *et al.*, Phys. Lett. **B 707** (2012) 6; Nucl. Phys. **B 867** (2013) 244.
- [6] A. D. Martin *et al.*, Eur. Phys. J. **C 64** (2009) 653; Eur. Phys. J. **C 73** (2013) 2318.
- [7] G. Watt, JHEP **1109**, 069 (2011).
- [8] S. Forte and G. Watt, Ann. Rev. Nucl. Part. Sci. **63**, 291 (2013).
- [9] S. Alekhin, J. Blumlein and S. Moch, Phys. Rev. **D 86** (2012) 054009.
- [10] R. S. Thorne, Eur. Phys. J. **C 74**, 2958 (2014).
- [11] BCDMS Collab., A.C. Benevenuti *et al.*, Phys. Lett. **B 223** (1989) 485; Phys. Lett. **B 237** (1990) 592; Phys. Lett. **B 195** (1987) 91.
- [12] V. Genchev *et al.*, *in* Proc. Int. Conference of Problems of High Energy Physics (1988), Dubna, V.2., p.6.
- [13] V. G. Krivokhizhin and A. V. Kotikov, Phys. Atom. Nucl. **68** (2005) 1873 [Yad. Fiz. **68** (2005) 1935].
- [14] SLAC Collab., L.W. Whitlow *et al.*, Phys. Lett. **B282** (1992) 475; L.W. Whitlow, Ph.D. Thesis Stanford University, SLAC report 357 (1990).
- [15] NM Collab., M. Arneodo *et al.*, Nucl. Phys. **B 483** (1997) 3.
- [16] J.A.M. Vermaseren, A. Vogt and S. Moch, Nucl.Phys.**B 688** (2004) 101.
- [17] V. G. Krivokhizhin and A. V. Kotikov, Phys. Part. Nucl. **40** (2009) 1059.
- [18] M. Virchaux and A. Milsztajn, Phys. Lett. **B 274** (1992) 221.
- [19] V.N. Gribov and L.N. Lipatov, Sov. J. Nucl. Phys. **15** (1972) 438; L.N. Lipatov, Sov. J. Nucl. Phys. **20** (1975) 94; G. Altarelli and G. Parisi, Nucl. Phys. **B 126** (1977) 298; Yu.L. Dokshitzer, JETP **46** (1977) 641.
- [20] G. Parisi and N. Surlas, Nucl. Phys. **B 151** (1979) 421; I.S. Barker *et al.*, Nucl. Phys. **B 186** (1981) 61; Z. Phys. **C 19** (1983) 147; Z. Phys. **C 24** (1984) 255.
- [21] V.G. Krivokhizhin *et al.*, Z. Phys. **C 36** (1987) 51; Z. Phys. **C 48** (1990) 347.
- [22] D.I. Kazakov and A.V. Kotikov, Nucl.Phys. **B 307** (1988) 791; (E: **345**, 299 (1990)); A. V. Kotikov, Phys. Atom. Nucl. **57** (1994) 133 [Yad. Fiz. **57** (1994) 142]; A.V. Kotikov and V.N. Velizhanin, hep-ph/0501274.
- [23] G. Parente, A.V. Kotikov and V.G. Krivokhizhin, Phys. Lett. **B 333** (1994) 190.
- [24] F.J. Yndurain, Phys. Lett. **B 74** (1978) 68.
- [25] A. Gonzalez-Arroyo, C. Lopez, Nucl.Phys. **B 166** (1980) 429; A. Gonzalez-Arroyo, C. Lopez, F.J. Yndurain, Nucl.Phys. **B 174** (1980) 474.
- [26] A.L. Kataev *et al.*, Phys. Lett. **B 388** (1996) 179; Phys. Lett. **B 417** (1998) 374; Nucl. Phys. **B 573** (2000) 405; A.V. Sidorov, Phys. Lett. **B 389** (1996) 379.

- [27] A.L. Kataev, G. Parente and A.V. Sidorov, Phys. Part. Nucl. **34** (2003) 20.
- [28] J. Blumlein, H. Bottcher, A. Guffanti, Nucl.Phys. **B 774** (2007) 182.
- [29] V.I. Vovk, Z. Phys. **C 47** (1990) 57; A.V. Kotikov, G. Parente and J. Sanchez Guillen, Z. Phys. **C 58** (1993) 465.
- [30] F. James and M. Ross, “MINUIT”, CERN Computer Center Library, D 505, Geneve, 1987.
- [31] S. Alekhin, J. Bluemlein, L. Caminadac, K. Lipka, K. Lohwasser, S. Moch, R. Petti and R. Placakyte, Phys. Rev. D **91** (2015) 9, 094002 [arXiv:1404.6469 [hep-ph]].
- [32] M. Gockeler *et al.* [QCDSF and UKQCD Collaborations], PoS LATTICE **2010** (2010) 165 [arXiv:1101.2806 [hep-lat]].
- [33] Y. Aoki, T. Blum, H. W. Lin, S. Ohta, S. Sasaki, R. Tweedie, J. Zanotti and T. Yamazaki, Phys. Rev. D **82** (2010) 014501 [arXiv:1003.3387 [hep-lat]].
- [34] J. D. Bratt *et al.* [LHPC Collaboration], Phys. Rev. D **82** (2010) 094502 [arXiv:1001.3620 [hep-lat]].
- [35] C. Alexandrou, J. Carbonell, M. Constantinou, P. A. Harraud, P. Guichon, K. Jansen, C. Kallidonis and T. Korzec *et al.*, Phys. Rev. D **83** (2011) 114513 [arXiv:1104.1600 [hep-lat]].
- [36] S. Dinter, C. Alexandrou, M. Constantinou, V. Drach, K. Jansen, D. Renner, C. Alexandrou and M. Constantinou, PoS LATTICE **2010** (2010) 135 [arXiv:1101.5540 [hep-lat]].
- [37] S. Dinter, C. Alexandrou, M. Constantinou, V. Drach, K. Jansen and D. B. Renner, Phys. Lett. B **704** (2011) 89 [arXiv:1108.1076 [hep-lat]].
- [38] G. S. Bali, S. Collins, M. Deka, B. Glassle, M. Gockeler, J. Najjar, A. Nobile and D. Pleiter *et al.*, Phys. Rev. D **86** (2012) 054504 [arXiv:1207.1110 [hep-lat]].
- [39] J. R. Green, M. Engelhardt, S. Krieg, J. W. Negele, A. V. Pochinsky and S. N. Syritsyn, Phys. Lett. B **734** (2014) 290 [arXiv:1209.1687 [hep-lat]].
- [40] C. Alexandrou, EPJ Web Conf. **73** (2014) 01013 [arXiv:1404.5213 [hep-lat]].
- [41] W.L. van Neerven and A. Vogt, Nucl. Phys. **B 568** (2000) 263; **B 603** (2001) 42.
- [42] CMS Collab., S. Chatrchyan *et al.* Phys. Lett. **B 728** (2014) 496; Eur. Phys. J. **C 73** (2013) 2604; K. Rabbertz arXiv:1312.5694 [hep-ex].
- [43] B. Malaescu and P. Starovoitov, Eur. Phys. J. **C 72** (2012) 2041
- [44] J. Rojo, arXiv:1410.7728 [hep-ph].
- [45] A. Bazavov *et al.* Phys. Rev. **D 86** (2012) 114031.
- [46] Particle Data Group Collab., K. A. Olive *et al.* Chin. Phys. **C 38** (2014) 090001.
- [47] J.A.M. Vermaseren, A. Vogt and S. Moch, Nucl. Phys. **B 724** (2005) 3.
- [48] G. Grunberg, Phys. Lett. **B 95** (1980) 70; Phys. Rev. **D 29** (1984) 2315.
- [49] A. V. Kotikov, A. V. Lipatov and N. P. Zotov, J. Exp. Theor. Phys. **101** (2005) 811 [Zh. Eksp. Teor. Fiz. **128** (2005) 938].
- [50] D.V. Shirkov and I.L. Solovtsov, Phys. Rev. Lett. **79** (1997) 1209.
- [51] G. Cvetic, A. Y. Illarionov, B. A. Kniehl and A. V. Kotikov, Phys. Lett. **B 679** (2009) 350; A. V. Kotikov and B. G. Shaikhatdenov, Phys. Part. Nucl. **44** (2013) 543.

- [52] R.S. Pasechnik *et al.*, Phys. Rev. **D 78** (2008) 071902; Phys. Rev. **D 81** (2010) 016010; V. L. Khandramai et al., Phys. Lett. **B 706** (2012) 340; A. V. Kotikov, V. G. Krivokhizhin and B. G. Shaikhatdenov, Phys. Atom. Nucl. **75** (2012) 507; A. V. Sidorov and O. P. Solovtsova, Mod.Phys.Lett. **A 29** (2014) 1450194.